
1 The relative importance of antecedent soil moisture and precipitation
2 in flood generation in the middle and lower Yangtze River basin

3

4 Qihua Ran¹, Jin Wang², Xiuxiu Chen², Lin Liu², Jiyu Li², Sheng Ye^{2*}

5

6 ¹ State Key Laboratory of Hydrology-Water Resources and Hydraulic Engineering,
7 Hohai University, Nanjing 210098, China

8 ² Institute of Water Science and Engineering, College of Civil Engineering and
9 Architecture, Zhejiang University, Hangzhou 310058, China

10

11 * Corresponding author: Sheng Ye

12

13 Email address of the corresponding author: yesheng@zju.edu.cn

14

15 September 8, 2022

16

17

18

19 **Abstract**

20 Floods have caused severe environmental and social economic losses worldwide in
21 human history, and are projected to exacerbate due to climate change. Many floods are
22 caused by heavy rainfall with highly saturated soil, however, the relative importance of
23 rainfall and antecedent soil moisture and how it changes from place to place has not
24 been fully understood. Here we examined annual floods from more than 200
25 hydrological stations in the middle and lower Yangtze River basin. Our results indicate
26 that the dominant factor of flood generation shifts from rainfall to antecedent soil
27 moisture with the increase of watershed area. The ratio of the relative importance of
28 antecedent soil moisture and daily rainfall (SPR) is positively correlated with
29 topographic wetness index and has a negative correlation with the magnitude of annual
30 floods. This linkage between watershed characteristics that are easy to measure and the
31 dominant flood generation mechanism provides a framework to quantitatively estimate
32 potential flood risk in ungauged watersheds in the middle and lower Yangtze River
33 basin.

34 **Key words:** flood generation, scaling effect, topographic wetness index

35

36

37 **1. Introduction**

38 Flooding is one of the most destructive and costly natural hazards in the world, resulting
39 in considerable fatalities and property losses (Suresh et al., 2013). River floods have
40 affected nearly 2.5 billion people between 1994 and 2013 worldwide (CRED, 2015),
41 and caused 104 billion dollars losses every year (Desai et al 2015). The damages may
42 be further exacerbated by increasing frequency and intensity of extreme rainfall events
43 according to climate change projections (IPCC 2012; Ohmura and Wild 2002). Flood
44 control infrastructures and more accurate predictions are needed to reduce flood
45 damages, which requires better understanding of the underlying mechanism of flood
46 generation as well as the drivers of change (Villarini & Wasko 2021).

47 Numerous studies have been conducted to investigate the cause of floods across
48 the world (Bloschl et al 2013; Munoz et al 2018; Zhang et al 2018). Many studies
49 focused on examining the environmental and social characteristics that lead to specific
50 catastrophic flood events (Bloschl et al 2013; Liu et al 2020; Zhang et al., 2018). Others
51 concentrated on single locations, usually catchment outlets, to explore the influential
52 factors of floods and the future trends (Brunner et al., 2016; Munoz et al 2018). Yet
53 given the amount of data and time required, it is not practical to apply these detailed
54 studies to hundreds of catchments to generate an overview of the flood generation
55 mechanism at large scale.

56 Recently, researchers started to investigate the dominant flood generation
57 mechanisms at regional scales (Berghuijs et al 2019b; Do et al 2020; Garg & Mishra
58 2019; Smith et al 2018; Trambly et al 2021; Ye et al 2017). Most of these studies are
59 conducted in North America and Europe with well-documented long-term records
60 (Berghuijs et al 2016; Bloschl et al 2019; Do et al 2020; Musselman et al 2018; Rottler

61 et al 2020). Some research was conducted in China recently (Yang et al 2019; Yang et
62 al 2020), though such kind of work is still limited, further investigations are needed
63 given the considerable spatial heterogeneity and complexity in flood generation.

64 As the largest river in China, Yangtze River basin has long suffered from floods. In
65 summer 2020, 378 tributaries of the Yangtze River had floods exceeding the alarm level,
66 causing billions of dollars damage (Xia et al., 2021). With the increasing public
67 awareness, more accurate prediction is needed, which relies on better understanding.
68 However, due to the limitation of observations, there are only a few regional studies of
69 the flood generation mechanism in China, with few in the Yangtze River basin (Zhang
70 et al 2018; Yang et al 2019; Yang et al 2020). The large number of dams and reservoirs
71 built along the river further complicated the situation (Feng et al., 2017; Qian et al 2011;
72 Yang et al 2019).

73 Because of the relatively warm temperature, snowmelt has little impact on flood
74 generation in the Yangtze River basin (Yang et al 2020). Floods in the Yangtze River
75 basin usually occur during summer with relatively wet soil and high rainfall (Wang et
76 al 2021). Heavy rainfall with high antecedent soil moisture has also been identified as
77 dominant driver of floods across world (Beighuijs et al 2019b; Garg et al 2019;
78 Trambly et al 2021; Wasko et al 2020). Recently, studies started to examines the
79 relative importance of rainfall and antecedent soil moisture in flood generation
80 (Brunner et al., 2021; Wasko et al., 2021; Bennett et al., 2018; Bertola et al., 2021).
81 Quantitative evaluation of the relative contribution of rainfall and antecedent soil
82 moisture and its change across watersheds is still limited and currently unavailable in
83 China (Liu et al., 2021; Wu et al., 2015).

84 Based on the watersheds in the middle and lower Yangtze River basin, this study

85 attempts to explore the following questions: 1) is there a way to quantitatively describe
86 the relative importance of antecedent soil moisture and rainfall on flood generation; and
87 2) how would this combination of flood-generation rainfall and soil moisture vary
88 across watersheds, and what are the influential factors. Based on the observations and
89 model estimation (Section 2), the spatial distribution patterns of antecedent soil
90 moisture and rainfall were obtained and analyzed to investigate their individual
91 contribution to flood generation and the influential factors (Section 3). This allows for
92 further examination of the relative importance of antecedent soil moisture and rainfall
93 on flood generation and its linkage to watershed characteristics as well as its
94 implications to flood prediction (Section 4), all the results are summarized in Section 5.

95 **2 Methods**

96 **2.1 Study area**

97 The Yangtze River is the largest river in China, with a total length of 6,300 kilometers
98 and annual discharge of 920km^3 at the outlet (Yang et al., 2018). It drains through an
99 area of $1.8 \times 10^6 \text{ km}^2$, lying between $90^\circ 33'$ and $122^\circ 25'$ E and $24^\circ 30'$ and $35^\circ 45'$ N, and
100 is home to over 400 million people, most of which live in the middle and lower Yangtze
101 River basin (YZRB) (Cai et al., 2020). The elevation of the YZRB declines from west
102 to east: from over 3000m in Qinghai-Tibet Plateau, to around 1000m in the central
103 mountain region, and the 100m in Eastern China Plain (Wang et al., 2013). The
104 vegetation types in the YZRB are forests, shrubs, grassland and agricultural land,
105 accounting for 11.85%, 12.65%, 32.26% and 42.88% respectively. Grassland and
106 shrubs are the dominant vegetation in the middle and upper YZRB, while the
107 downstream YZRB is dominated by forests and agricultural land (Miao et al., 2010).
108 There are more than 51,000 reservoirs of different sizes in the whole basin, including

109 280 large ones (Peng et al., 2020).

110 Most of the YZRB is semi-humid and humid, with a typical subtropical monsoon
111 climate. The mean annual temperature is approximately 13.0 °C, varying from -4 °C
112 to 18°C downstream. The mean annual precipitation of the whole basin is about 1200
113 mm, increasing from 300mm in the western headwaters to 2400 mm downstream. (Li
114 et al., 2021). Most of the precipitation comes between June and September, the premise
115 of persistent heavy rain in the Yangtze River basin is the frequent activity of weak cold
116 air in the north (Tao et al., 1980) and the intersection of mid-latitude air mass and
117 monsoon air mass (Kato et al., 1985). Studies have found that both annual precipitation
118 and the frequency of extreme precipitation events have increased in the middle and
119 lower reaches of the Yangtze River (Qian et al., 2020; Fu et al., 2013). As a result, floods
120 have occurred frequently in the middle and lower reaches of the Yangtze River, where
121 most of the population in the YZRB live (Liu et al., 2018).

122 **2.2 Data**

123 In this work, we focus on the middle and lower reaches of the Yangtze River for the
124 high population density and increasing flood risk. The 30-meter digital elevation model
125 (DEM) was downloaded from Geospatial Data Cloud (<http://www.gscloud.cn/>), from
126 which the drainage area corresponding to the hydrological station was extracted by
127 ArcGIS. Daily precipitation data and temperature data between 1970 and 2016 from
128 247 meteorological stations within and near the YZRB were downloaded from China
129 Meteorological Data Network (<https://data.cma.cn/>) (Figure 1). The temperature data
130 was used to estimate potential evaporation. The observed precipitation and estimated
131 potential evaporation were interpolated into the whole YZRB using the Thiessen
132 polygon method (Meena et al., 2013). The interpolated precipitation and potential

133 evaporation were then averaged for the drainage area corresponding to each
134 hydrological station.

135 The daily streamflow data was collected from 267 hydrological stations from
136 Annual Hydrological Report of the People's Republic of China. Among which, 224
137 stations with at least 20 years records from both the period from 1970 to 1990 and the
138 period from 2007 to 2016 were selected, the data from 1990 to 2007 were not found in
139 online repository (see Figure S1 for data availability). Information of 361 reservoirs in
140 the middle and lower YZRB, including capacity and controlling area was downloaded
141 and extracted from the Global Reservoir and Dam database (GRanD) (Lehner et al
142 2011). Previous study showed that this database provides reliable information of middle
143 and large reservoirs in China (Yang et al 2021). Watersheds with more than 80% of the
144 drainage area under control reservoirs according to GRanD database and/or located
145 right downstream of reservoirs and water gates were considered as watersheds under
146 strong regulation (regulated watersheds).

147 **2.3 Calculation of hydrological and topographic characteristics**

148 *Potential evaporation estimation*

149 The temperature data was used to estimate potential evaporation following the
150 Hargreaves method (Allen et al., 1998; Vicente et al., 2014; Berti et al., 2014).

$$151 \quad ET_0 = 0.0023 \times (T_{max} - T_{min})^{0.5} \times (T_{mean} + 17.8) \times Ra \quad (1)$$

152 where ET_0 is potential evaporation (mm/d), T_{max} is the highest temperature ($^{\circ}\text{C}$), T_{min}
153 is the lowest temperature ($^{\circ}\text{C}$), T_{mean} is the mean temperature ($^{\circ}\text{C}$), and Ra is the outer
154 space radiation [$\text{MJ}/(\text{m}^2 \cdot \text{d})$], which can be calculated as follows:

155
$$Ra = 37.6 \times d_r \times (\omega_s \sin \varphi \sin \delta + \cos \varphi \cos \delta \sin \omega_s), \quad (2)$$

156 where d_r is the reciprocal of the relative distance between the sun and the earth, ω_s is
157 the angle of sunshine hours, δ is the inclination of the sun (rad), φ is geographic
158 latitude (rad). d_r , δ and ω_s can be calculated by the following formula:

159
$$d_r = 1 + 0.033 \times \cos\left(\frac{2\pi J}{365}\right), \quad (3)$$

160
$$\delta = 0.409 \times \sin\left(\frac{2\pi J}{365} - 1.39\right), \quad (4)$$

161
$$\omega_s = \arcsin(-\tan \varphi \tan \delta), \quad (5)$$

162 where J is the daily ordinal number (January 1st is 1).

163 *Soil water storage estimation*

164 The soil water storage was estimated based on the daily water balance (Berhuijs et al.,
165 2016, 2019):

166
$$\frac{dS}{dt} = P - ET - \max(Q, 0), \quad (6)$$

167 Where S is the soil water storage (mm), which is initially set to 0. Due to the long term
168 of simulation, the change of initial value would not significantly affect the results. P is
169 precipitation (mm/d), Q is discharge normalized by area (mm/d), ET is evaporation
170 (mm/d), which can be calculated from potential evapotranspiration (ET_0), where the
171 soil water storage (S) is used as the upper limit of daily ET:

172
$$ET = \min(0.75 \times ET_0, S), \quad (7)$$

173 The estimation of soil water storage and ET are highly simplified and is not used for

174 prediction but to capture the first order of the temporal variation and the relative
175 wetness of soil in the study time period, which helps develop a framework that
176 differentiates the relative contribution of precipitation and soil moisture in flood
177 generation.

178 *Topographic wetness index estimation*

179 Topographic wetness index was calculated to represent the combined impacts of
180 drainage area and topographic gradient (Alfonso et al., 2011; Grabs et al., 2009):

$$181 \qquad \qquad \qquad TWI = \ln(A_d/\tan\alpha), \qquad \qquad \qquad (8)$$

182 where A_d is drainage area and α is topographic gradient estimated from DEM. TWI
183 represents the propensity of subsurface flow accumulation and frequency of saturated
184 conditions, thus can be used to predict relative surface wetness and hydrological
185 responses (Meles et al 2020). It is widely used to quantify topographic impact on
186 hydrological processes (i.e., spatial scale effects, hydrological flow path, etc.), as well
187 as in land surface models for hydrological, biogeochemical and ecological processes
188 (Sorensen et al 2006).

189 **2.4 Quantification of the relative importance of soil moisture and precipitation** 190 **during floods**

191 The maximum daily discharge of each year was selected as annual flood, which was
192 then averaged across years as the mean annual maximum flood (AMF). The observed
193 rainfall on that day and the estimated soil water storage at the day before AMF in each
194 year were also averaged across years as daily rainfall (P) and antecedent soil moisture
195 (S_0). Since almost all the AMFs in our study region come during rainy season when
196 rainfall comes in most of the days, it could be difficult to isolate the events of AMFs

197 among consecutive flow events. To avoid the bias that may be caused in event
198 separation, the soil moisture at the day before AMF was used as antecedent soil
199 moisture, instead of the day before the event of AMF. To examine the impacts from
200 long-lasting rainfall event, especially for the large watersheds with longer concentration
201 time, we also calculated the mean accumulated rainfall from two days (rainfall on the
202 flood day and the day before, P_2) to seven days before (weekly rainfall, P_7).

203 The percentile of antecedent soil moisture (S_0) was calculated to represent the
204 relative saturation of soil moisture in the time series; while the percentile of daily
205 rainfall (P) was estimated to show the relative intensity (P'), representing the relative
206 magnitude of rainfall events across time. The percentile of accumulated rainfall was
207 also calculated for the two-day to seven-day rainfall.

208 To quantify the relative importance of antecedent soil moisture and rainfall in flood
209 generation, the ratio between these two factors at the AMFs was derived: $SPR = S'/P'$.
210 When SPR is large, the antecedent soil moisture is much closer to the maximum, while
211 the daily rainfall is less extreme, floods are more affected by the antecedent soil
212 moisture. On the other hand, a smaller SPR indicates relatively larger magnitude of
213 rainfall comparing with antecedent soil moisture, that is, rainfall is more extreme and
214 influential in flood generation.

215 **3 Results**

216 **3.1 Spatial patterns of antecedent soil moisture and precipitation during floods**

217 Figure 2 shows the spatial distribution of the percentile of antecedent soil moisture and
218 daily rainfall during the annual maximum floods (AMFs) in the middle and lower
219 reaches of the Yangtze River. As we can see from Figure 2a, in the middle and lower

220 reaches of YZRB, when AMFs occurred, the percentile of antecedent soil saturation
221 was generally high, most of them are larger than 0.6: the farther away from the main
222 stream, the more saturated the soil was. On the other hand, along and near the main
223 stream and the delta, the antecedent soil saturation rate could be much smaller, even
224 less than 0.4.

225 Figure 2b shows the daily rainfall during the AMFs. As we can see, the percentile
226 of daily rainfall is relatively high (>0.8) at more than half of the study sites, while it is
227 small (<0.5) for the sites along the main stream and in the delta (Figure 2b). Comparison
228 between Figure 2a and b suggests that, except the sites on the main stream and in the
229 delta, sites with relatively high antecedent soil saturation rate (i.e., >0.8 , the blue dots)
230 during AMFs are also the ones with relatively small daily rainfall contribution (i.e.,
231 <0.8 , the light blue and cyan dots). That is, for these sites, the AMFs are usually
232 occurring at a much wetter condition while extreme rainfall at flood day is not necessary,
233 suggesting the relative importance of soil wetness. For the sites with both the percentile
234 of soil moisture and rainfall between 0.6 and 1, both the antecedent soil moisture and
235 rainfall play important roles in flood generation. As for the sites on the main stream and
236 in the delta, both antecedent soil moisture and rainfall are low during AMFs, this is
237 likely due to the regulations from large reservoirs and water gates.

238 **3.2 The scaling effect in the contribution of antecedent soil moisture and rainfall**

239 To further investigate the relative importance of antecedent soil moisture and rainfall
240 in flood generation and the potential influential factors, we examined their correlation
241 with catchment area (Figure 3). Given the complicated environmental and social
242 impacts, the regulated watersheds and sites on the main stream are presented separately
243 (the green dots and cyan dots in Figure 3 respectively). Our study will focus on the sites

244 that are not dominated by regulation (the blue dots in Figure 3), for simplicity, we will
245 refer them as natural watersheds.

246 As we can see from Figure 3, during the occurrence of AMFs, the percentile of
247 antecedent soil wetness increases with watershed area (p -value <0.001), while the
248 percentile of daily rainfall decreases with watershed area (p -value <0.001). That is, with
249 the increase of watershed size, antecedent soil moisture becomes more and more
250 saturated while the precipitation is less and less extreme during AMFs; suggesting the
251 rising contribution of antecedent soil moisture and declining importance of daily
252 precipitation in flood generation. As for the regulated watersheds (green dots in Figure
253 3), there is no clear correlation between drainage area and the percentile of antecedent
254 soil moisture or rainfall, which is understandable. Meanwhile, both the percentile of
255 antecedent soil moisture and rainfall decreases with watershed area for main stream
256 sites.

257 **3.3 The scaling impacts on accumulated rainfall**

258 The saturation of soil before floods could be due to previous rainfall events, and could
259 also be caused by accumulated rainfall in long-lasting rainfall events that eventually
260 generate floods (Xie et al., 2018). Figure 4 presents the correlation between the
261 percentile of accumulated rainfall and drainage area. When single day rainfall is
262 considered, it is negatively correlated with drainage area (Figure 3a); when
263 accumulated rainfall is considered, the correlation gradually shifts from negative to
264 positive correlation (Figure 4). For example, when two-day rainfall was examined, the
265 correlation between accumulated rainfall and drainage area shifts from negative to
266 positive at 10,000 km²; the negative correlation in Figure 3a is only valid for watersheds
267 larger than 10,000 km² (Figure 4a). This transition area increases from 10,000 km² for

268 two-day rainfall to 100,000 km² for four-day rainfall (Figure 4c). The number of
269 watersheds with negative correlation also decreases. Eventually, the weekly rainfall has
270 similar positive correlation with drainage area like antecedent soil moisture (Figure 4f).
271 The increase of transition area may be explained by the increasing response time and
272 confluence time in large watersheds: it takes days to generate flow events by heavy
273 rainfall and for them to reach outlets where it can be observed in large watersheds. This
274 is also consistent with the conclusion in the Yellow River Basin (Ran et al., 2020) and
275 our previous findings of the dominant flood generation mechanism in the middle and
276 lower YZRB: weekly rainfall is the dominant flood driver for sites on the main streams
277 and the major tributaries (Wang et al 2021). The regulated watersheds don't show
278 significant correlation which is understandable for the strong human intervention. For
279 the negative correlation between accumulated rainfall and drainage area at main stream
280 sites, it is difficult to decide whether it is due to scaling effect or human intervention.

281 **3.4 The interlink of watershed characteristics, flood, antecedent soil moisture and** 282 **rainfall**

283 Figure 5 presents the percentile of antecedent soil moisture and rainfall during the
284 AMFs at the study watersheds, the circles are scaled by watershed size and colored with
285 topographic gradient. Except the watersheds with strong human intervention (regulated
286 ones and the ones on main stream), there is a negative correlation between the
287 contribution of rainfall and antecedent soil moisture. The lower right of the scatter are
288 mostly big blue dots, which are large watersheds with gentle topographic gradient. That
289 is, AMFs usually occur when soil moisture is close to saturation while extreme rainfall
290 is not necessary for AMFs in these watersheds. On top of the scatter are relatively small
291 yellow and green dots, those are medium to small watersheds with steep topographic

292 gradient. That is, AMFs are usually generated with extreme rainfall, while the saturation
293 of soil moisture is not necessary. This negative correlation indicates the shift of
294 dominance in AMFs generation from extreme rainfall to antecedent soil wetness from
295 small steep watersheds to large flat ones.

296 Figure 6 shows the relative importance of antecedent soil moisture and rainfall. For
297 the natural watersheds (the circles), SPR increases with drainage area and declines with
298 topographic gradient. That is, the larger the drainage area is, the more essential the
299 contribution of antecedent soil moisture to floods is, and the less influential rainfall is
300 in flood generation. For watersheds with similar drainage area (i.e., the green or light
301 blue dots in Figure 6b), topographic gradient also cast impacts on SPR: SPR decreases
302 with slope. That is, the relative importance of rainfall increases at steeper watersheds.
303 This may be attributed to the shortened hydrological response time due to the steep
304 topography which facilitates rainfall induced floods generation. As a combination of
305 both drainage area and topographic gradient, TWI is positively correlated with SPR at
306 natural watersheds, with less scatter than the correlation between SPR and drainage
307 area or topographic gradient alone. That is, watersheds with larger area and gentler
308 topographic gradient that are easier to get wet tend to have larger SPR: soil wetness is
309 more important in flood generation. There is no significant correlation between SPR
310 and TWI for the regulated watersheds along tributaries (black triangles). However, the
311 sites on main stream show opposite pattern: the SPR at these sites decreases with TWI
312 and drainage area. It is difficult to determine whether this is because of reservoir
313 regulation or not. More data about watersheds larger than 10,000km² but with limited
314 human intervention are needed to examine this hypothesis.

315 Besides TWI, SPR is also correlated with the magnitude of AMF (Figure 7). As

316 Figure 7 shows, the area normalized flood peak declines with flood-generation SPR.
317 Watersheds with large flood peak are mostly the ones with steep topographic gradient
318 and small SPR (i.e., $SPR < 1$) and vice versa. Catchments with more extreme floods are
319 the ones with relatively less influence of soil moisture on flood generation. Similar
320 correlation was also found at event scale in our experimental mountainous watershed,
321 which locates at a headwater of Yangtze River (Liu et al 2021).

322 **4 Discussion**

323 **4.1 The relative importance of antecedent soil moisture and rainfall in flood** 324 **generation**

325 While soil moisture and rainfall are the two main drivers of floods in the middle and
326 lower Yangtze River basin, the dominance of each factor varies across the relatively
327 natural watersheds. Floods in large watersheds are usually generated when soil is almost
328 saturated despite of the relatively small rainfall amount, while extreme rainfall is
329 usually observed during floods in small to medium watersheds (blue dots in Figure 3).
330 The rising contribution of antecedent soil moisture in large watersheds was consistent
331 with the findings in Australian watersheds (Wasko & Nathan, 2019); and the declining
332 influence of rainfall at larger watersheds was also found in Indian watersheds (Garg et
333 al 2019). This contrast correlation with watershed size indicates a shift of dominance
334 in AMFs generation, which may be attributed to the longer confluence time in the large
335 watersheds and less heterogeneity in small watersheds.

336 This shift of dominance can be observed more straightforwardly from the negative
337 correlation between the percentile of rainfall and antecedent soil moisture in Figure 5.
338 The natural watersheds in Figure 5 could be grouped into three classes based on their

339 drainage area and topographic gradient. When a watershed is large and flat, flood
340 occurrence is mainly determined by soil wetness (i.e., the big blue dots at the lower
341 right of the scatter); on the other hand, when a watershed is small and steep, heavy
342 rainfall takes over the dominance (i.e., the small yellow and green dots at the upper left
343 of the scatter). Between these two groups are relatively small watersheds with gentle
344 topographic gradient, where the occurrence of AMF requires both highly saturated soil
345 and relatively heavy rainfall. That is, the dominant influential factor(s) in AMFs
346 generation across watersheds is correlated with the topographic characteristics (i.e.,
347 watershed size and topographic gradient). This helps quantify the relative importance
348 of soil moisture and rainfall in flood generation in the existing work.

349 This shift of dominance is not observed in the main stream sites (i.e., cyan dots in
350 Figure 3), where the percentile of both antecedent soil moisture and precipitation
351 declines with drainage area. This may be attributed to the more complicated flood
352 generation mechanism at large scale as well as the strong human intervention on main
353 stream (e.g., reservoirs, water gates regulation, etc.) (Gao et al., 2018; Long et al., 2020;
354 Zhang et al., 2017). The major responsibilities of reservoirs on the main stream are to
355 reduce peak flow and postpone the time to flood peak (Volpi et al., 2018). As a result,
356 the original flood peak would be delayed by regulation and the actual flood peak would
357 occur when rainfall declines/stops and soil water drains. Another possibility is that
358 when watershed size is larger than 100,000km², the impact of antecedent soil moisture
359 declines as well. To examine this hypothesis, more data from watersheds larger than
360 100,000km² and with limited human intervention is needed. However, this is above the
361 scope of this work and requires future studies.

362 **4.2 Linkage between topographic characteristics, SPR and floods**

363 The correlation between TWI and SPR (Figure 6c) demonstrates that the relative
364 importance of soil moisture and rainfall could be inferred from topographic
365 characteristics quantitatively. We could derive the relative dominance of soil moisture
366 and rainfall in flood generation in specific watershed from its TWI for the natural
367 watersheds without significant human intervention. Rainfall and soil moisture level
368 have been identified as dominant drivers of floods, individually or together, in
369 watersheds worldwide (Berghuijs et al 2016, 2019b; Garg & Mishra 2019; Trambly et
370 al 2021; Ye et al 2017). Our findings provide a framework to quantify the relative
371 importance of rainfall and soil moisture and to further identify the influential factors of
372 their importance based on topographic characteristics that are easy to measure.

373 Meanwhile, the SPR also present a negative correlation with the magnitude of
374 AMFs (Figure 7). That is, we could infer the mean annual AMF based on SPR for each
375 watershed. Since the characteristic SPR could be estimated from TWI, we could derive
376 quantitative estimation of the mean AMFs from topographic characteristics that are
377 easy to measure, even in watersheds with little hydrologic records. There is also similar
378 negative correlation between TWI and AMFs (Figure S2). This would be helpful for
379 flood control management in ungauged watersheds, especially in the mountainous
380 watersheds with risks of flash floods. Similar correlation was also found in the
381 observations from our experimental watershed, a headwater of Yangtze River (Liu et al
382 2021). The ratio of observed antecedent soil moisture and event precipitation also
383 presents similar decline trend with discharge at event scale. However, the correlation
384 between SPR and discharge at event scale is preliminary, more data with higher
385 resolution and detailed analysis are needed for validation at event scale. For this study,
386 our goal is to present the framework to derive flood generation SPR that could be
387 estimated from topographic characteristics and to provide information of mean AMFs.

388 In conclusion, based on the topographic characteristics, we could derive the relative
389 importance of soil moisture and rainfall in flood generation (SPR); and from this
390 relative importance ratio, we could further infer the average flood magnitude at these
391 watersheds. As a result, we could link the topographic characteristics and annual floods
392 through the characteristic SPR during the AMFs.

393 **4.3 Implications**

394 Our findings could be helpful for potential flood risk evaluation in ungauged basins,
395 e.g., headwaters in the mountainous region. With the construction of large reservoirs,
396 the capability of flood risk control has improved substantially along the main stream
397 (Zou et al., 2011; Zhang et al., 2015). However, it is still difficult for quantitative
398 evaluation of flood risk in upstream mountainous watersheds, which are vulnerable to
399 floods but difficult for hydrological modeling and prediction due to little hydrologic
400 records.

401 Our findings suggest that we could derive the flood-generation SPR of each
402 watershed from drainage area and topographic gradient that are easy to measure. The
403 correlation between SPR and flood peak provides information of the mean annual
404 floods in ungauged watersheds. Therefore, in regions without observation data, to build
405 flood control infrastructure such as dams and gates, the mean annual flood peak
406 obtained by SPR based on the topographic characteristics can be used to provide
407 quantitative information for flood control and disaster management. Flood control
408 infrastructures could be designed based on the estimated mean annual flood peak as
409 well as the demographic information. With further validation of this framework at event
410 scale, by using the observed soil moisture from remote sensing data and precipitation
411 forecast to generate real-time prediction of SPR values, we could further provide early

412 warning of floods in these ungauged watersheds. This would be helpful given the
413 increasing possibility of extreme rainfall events due to climate change, however, more
414 data and examination are needed in future studies.

415 **4.4 Limitations**

416 Previous works usually identify the dominant flood generation mechanism based on the
417 comparison of the timing of events (Berghuijs et al 2016; 2019b; Bloschl et al 2017; Ye
418 et al 2017). Similar work has been implemented in our study watersheds, suggesting
419 the importance of soil moisture and rainfall (Wang et al 2021). Based on that, we further
420 looked into the records to quantitatively evaluate the relative importance of soil
421 moisture and rainfall in flood generation. However, there are limitations in our methods.

422 The precipitation data we used were averaged for the study watersheds from 247
423 meteorological stations. Given the large area and considerable spatial heterogeneity, the
424 precipitation data we used may not always be representative of the actual precipitation
425 events. The daily data could also average the rainfall intensity at hourly scale, which
426 could be influential in small mountainous watersheds. ET was scaled as $0.75 \cdot ET_0$ to
427 make sure it is smaller than the potential evaporation. This is a simplified estimation of
428 ET; more sophisticated method is needed in further analysis on specific catchments at
429 event scale.

430 The estimation of soil moisture is also highly simplified, which cannot be
431 considered as precise estimation at event scale. To reduce the influence from this
432 simplification, we used the percentile of soil moisture to represent the relative wetness
433 of soil moisture as well as the seasonal trend of soil moisture, which was then compared
434 with the percentile of rainfall (see supplementary and Figure S3, S4). While more

435 sophisticated models can be used for soil moisture estimation, there could still be
436 substantial uncertainties (Ran et al 2020). Yet the seasonal trend and the relative
437 magnitude, after averaging through long-term records would be less impacted by the
438 simplification in estimation (Berghuijs et al 2019; Zhang et al 2019).

439 Our findings may appear different from that in Yang et al (2020), which attributed
440 the dominant flood generation mechanism in the Yangtze River basin to rainfall. This
441 may be explained by different classification criteria: Yang et al (2020) considered both
442 short-rain and long-rain as rainfall impacts while here we only considered the daily
443 rainfall. Thus, the importance of antecedent soil moisture may be considered as long-
444 rain impacts in Yang et al (2020). It is possible that soil moisture at the day before the
445 AMFs may not be the soil moisture before the event in large catchments due to the long
446 concentration time. We estimated the concentration time for 10 sites with largest
447 drainage area (larger than 100,000 km²): the ones on the main stream and at the outlets
448 of major tributaries following the USBR method (USBR 1973; Gericke & Smithers
449 2014). The concentration time is mostly within two days for main stream sites and is
450 less than 24hr for sites at the outlets of major tributaries (Table S1). Since the rest of
451 the sites are all smaller than these ones, so would be the concentration time. That is, for
452 the natural watersheds we focused on, the concentration time is likely to be within one
453 day. Thus, the soil moisture at the day before AMFs would contribute to the generation
454 of AMFs, and should be applicable for this study.

455 Besides, the exchange with groundwater was not considered in the soil moisture
456 estimation. The exchange with groundwater is more complicated and heterogenous (i.e.,
457 rivers could receive groundwater recharge in hilly area and recharge groundwater in
458 lower land (Che et al 2021)). According to Huang et al. (2021), the variation of

459 groundwater level in the Yangtze River basin is relatively small. Since the goal of this
460 study is to capture the first order seasonal variation of soil moisture and develop a
461 framework that differentiates the relative importance of precipitation and soil moisture
462 in flood generation, in this study, we estimated the soil moisture following Berhuijs (et
463 al 2016, 2019) with a simple water balance equation.

464 Moreover, this work is focused on the relative importance soil moisture and rainfall,
465 the impact of snowmelt is not considered due to the warm and humid climate in the
466 study watersheds. To apply our findings to cold watersheds with significant impact of
467 snow, the snowmelt component needs to be incorporated. In addition, our method is
468 based on the average values from many years. While previous work indicated that the
469 occurrence of floods in our study watersheds are highly concentrated (Wang et al 2021),
470 there could be strong inter-annual variability in other watersheds. In future studies,
471 annual scale and event scale analysis are needed to examine and improve our findings
472 before it can be applied to watersheds with more diverse climate and landscape
473 conditions. There could be uncertainties embedded in the estimation of soil moisture
474 due to the uncertainties in the inputs and model structures. Comprehensive evaluation
475 of the performance and uncertainty is beyond the scope of our study. More sophisticated
476 models with groundwater component, remote sensing data, and reanalysis product with
477 higher spatial-temporal resolution are needed to provide more accurate estimation and
478 further validation of soil moisture, ET, and advances our understandings of the flood-
479 generation SPR.

480 **5 Conclusions**

481 Heavy rainfall on highly saturated soil was identified as the dominant flood generation
482 mechanism across world (Berghuijs et al 2019; Wang et al 2021; Wasko et al 2020).

483 This study aims to further evaluate the relative importance of antecedent soil moisture
484 and rainfall on floods generation and the controlling factors. Climate and hydrological
485 data from 224 hydrological stations and 247 meteorological stations in the middle and
486 lower reaches of the Yangtze River basin was analyzed, along with the modeled soil
487 moisture. Except the regulated watersheds, the relative importance of antecedent soil
488 moisture and daily rainfall present significant correlation with drainage area: the larger
489 the watershed is, the more essential antecedent soil saturation rate is in flood generation,
490 the less important daily rainfall is.

491 Using the percentile of antecedent soil moisture and rainfall as coordinates, the
492 flood generation mechanism(s) of study watersheds could be grouped into three classes:
493 antecedent soil moisture dominated large flat watersheds, heavy rainfall dominated
494 steep and small to middle size watersheds, and small to middle size watersheds with
495 gentle topographic gradient where floods occurrence requires both highly saturated soil
496 and heavy rainfall. Our analysis further shows that the ratio of relative importance
497 between antecedent soil moisture and rainfall (SPR) can be predicted by topographic
498 wetness index. When the topographic wetness index is large, the dominance of
499 antecedent soil moisture for extreme floods is stronger, and *vice versa*. The SPR also
500 presents negative correlation with area normalized flood peak.

501 With the potential increase of extreme rainfall events (Gao et al., 2016; Chen et
502 al., 2016), upstream mountainous watersheds in the middle and lower Yangtze River
503 basin are facing higher risk of extreme floods. The lack of hydrological records further
504 increases the vulnerability of people in these watersheds. The flood risks could be
505 reduced by construction of flood control facilities, but it is difficult to set flood control
506 standards in these ungauged watersheds. Our findings provide a framework to

507 quantitatively estimate the possible flood risk for these ungauged watersheds. Based on
508 measurable watershed characteristics (i.e., drainage area and topographic gradient), the
509 flood generation SPR could be derived, which could then be used to estimate the mean
510 annual flood. This information can provide scientific support for flood control
511 management as well as infrastructures construction.

512 Future analysis at event scale could help generate the flood-generation curve
513 between SPR and discharge at event scale to further improve flood risk predictions in
514 these small ungauged watersheds. With more data from other regions and improved
515 estimation or observation of soil moisture, we could expand our analysis to watersheds
516 with more diverse climate and topographic characteristics to examine and refine our
517 findings and to enhance our understandings of flood generation. Comparison between
518 different time periods (i.e., before and after 2000) could also reveal temporal changes
519 in [flood generation](#), which may be linked to [climate change](#), yet longer data records are
520 needed to [generate representative patterns](#).

521

522 **Data availability**

523 DEM data was downloaded from Geospatial Data Cloud at <http://www.gscloud.cn/>.
524 Climatological data used in this study was obtained from China Meteorological Data
525 Network, which can be accessed at <http://data.cma.cn/>. Discharge data comes from
526 Annual Hydrological Report of the People's Republic of China issued by Yangtze River
527 Water Resources Commission.

528

529 **Acknowledgements**

530 This research was funded by the National Key Research and Development Program of
531 China (2019YFC1510701-01), and National Natural Science Foundation of China
532 (51979243).

533

534 **References**

- 535 Abbas, S.A., Xuan, Y. and Song, X.: Quantile Regression Based Methods for
536 Investigating Rainfall Trends Associated with Flooding and Drought Conditions.
537 Water Resources Management, 33(12), 4249-4264, [https://doi:10.1007/s11269-](https://doi:10.1007/s11269-019-02362-0)
538 019-02362-0, 2019.
- 539 Alfonso R., Nilza M. R.C., and Anderson L. R.: Numerical Modelling of the
540 Topographic Wetness Index: An Analysis at Different Scales, International
541 Journal of Geosciences(4), 476-483, <https://doi:10.4236/ijg.2011.24050>, 2011.
- 542 Allen R. G., Pereira L. S. and Races D.: Crop evapotranspiration-Guidelines for
543 computing crop water requirements FAO Irrigation and drainage paper
544 NO.56(Electric Publication)[M], Rome , Italy:FAO, 1998.
- 545 Bennett, B., Leonard, M., Deng, Y., Westra, S.: An empirical investigation into the
546 effect of antecedent precipitation on flood volume. J. Hydrol. 567, 435–445.
547 <https://doi.org/10.1016/j.jhydrol.2018.10.025>, 2018.
- 548 Berghuijs, W.R., Allen, S.T., Harrigan, S. and Kirchner, J.W.: Growing Spatial Scales
549 of Synchronous River Flooding in Europe. Geophysical Research Letters, 46(3),
550 1423-1428, <https://doi:10.1029/2018GL081883>, 2019a.
- 551 Berghuijs, W.R., Harrigan, S., Molnar, P., Slater, L.J. and Kirchner, J.W.: The Relative
552 Importance of Different Flood-Generating Mechanisms Across Europe. Water
553 Resources Research, 55(6), 4582-4593, <https://doi:10.1029/2019WR024841>,
554 2019b.
- 555 Berghuijs, W.R., Woods, R.A., Hutton, C.J. and Sivapalan, M.: Dominant flood
556 generating mechanisms across the United States. Geophysical Research Letters,
557 43(9), 4382-4390, <https://doi:10.1002/2016GL068070>, 2016.
- 558 Bertola, M., Viglione, A., Vorogushyn, S., Lun, D., Merz, B., Blöschl, G.: Do small
559 and large floods have the same drivers of change? A regional attribution analysis
560 in Europe. Hydrol. Earth Syst. Sci. 25, 1347–1364. [https://doi.org/10.5194/hess-](https://doi.org/10.5194/hess-25-1347-2021)
561 25-1347-2021, 2021.
- 562 Blöschl, G., Nester, T., Komma, J., Parajka, J. and Perdigao, R.A.P.: The June 2013
563 flood in the Upper Danube Basin, and comparisons with the 2002, 1954, and 1899
564 floods. Hydrol. Earth Syst. Sci., 17, 5197–5212, 2013.

-
- 565 Blöschl, G., Hall, J., Parajka, J., Perdigão, R. A., Merz, B., Arheimer, B., et al.:
566 Changing climate shifts timing of European floods. *Science*, 357(6351), 588 –
567 590. <https://doi.org/10.1126/science.aan2506>, 2017.
- 568 Blöschl, G., Hall, J., Viglione, A., Perdigao, R.A., Parajka, J., Merz, B., et al.: Changing
569 climate both increases and decreases European river floods, *Nature*, 573, 108 –
570 111, 2019.
- 571 Berti, A., Tardivo, G., Chiaudani, A., Rech, F. and Borin, M.: Assessing reference
572 evapotranspiration by the Hargreaves method in north-eastern Italy. *Agricultural*
573 *Water Management*, 140, 20-25, <https://doi:10.1016/j.agwat.2014.03.015>, 2014.
- 574 Brunner, M. I., Seibert, J. and Favre, A.C.: Bivariate return periods and their importance
575 for flood peak and volume estimation. *Wire's Water*, 3, 819 – 833.
576 <https://doi.org/10.1002/wat2.1173>, 2016.
- 577 Brunner, M. I., Gilleland, E., Wood, A., Swain, D. L., and Clark, M.: Spatial
578 dependence of floods shaped by spatiotemporal variations in meteorological and
579 land - surface processes. *Geophysical Research Letters*, 47, e2020GL088000.
580 <https://doi.org/10.1029/2020GL088000>, 2020.
- 581 Brunner, M. I., Swain, D. L., Wood, R.R. et al. An extremeness threshold determines
582 the regional response of floods to changes in rainfall extremes. *Commun Earth*
583 *Environ* 2, 173. <https://doi.org/10.1038/s43247-021-00248-x>, 2021.
- 584 Cai, Q. H.: Great protection of Yangtze River and watershed ecology, *Yangtze River*
585 (01), 70-74, <https://doi:10.16232/j.cnki.1001-4179.2020.01.011>, 2020.
- 586 Cen, S.-x., Gong, Y.-f., Lai, X. and Peng, L.: The Relationship between the
587 Atmospheric Heating Source/Sink Anomalies of Asian Monsoon and
588 Flood/Drought in the Yangtze River Basin in the Meiyu Period. *Journal of*
589 *Tropical Meteorology*, 21(4), 352-360, 2015.
- 590 Che, Q., Su, X., Zheng, S., Li, Y.: Interaction between surface water and groundwater
591 in the Alluvial Plain (anqing section) of the lower Yangtze River Basin:
592 environmental isotope evidence. *Journal of Radioanalytical and Nuclear*
593 *Chemistry*, 329, 1331–1343, 2021.
- 594 Chen, Y. and Zhai, P.: Mechanisms for concurrent low-latitude circulation anomalies
595 responsible for persistent extreme precipitation in the Yangtze River Valley.

596 Climate Dynamics,47(3-4), 989-1006, <https://doi:10.1007/s00382-015-2885-6>,
597 2016.

598 CRED (2015). The human cost of natural disasters: A gobal perspective: Centre for
599 research on the epidemiology of disasters.

600 Deb, P., Kiem, A.S. and Willgoose, G.: Mechanisms influencing non-stationarity in
601 rainfall-runoff relationships in southeast Australia. *Journal of Hydrology*, 571,
602 749-764, <https://doi:10.1016/j.jhydrol.2019.02.025>, 2019.

603 Desai, B., Maskrey, A., Peduzzi, P., De Bono, A., & Herold, C. Making Development
604 Sustainable: The Future of Disaster Risk Management. Global Assessment Report
605 on Disaster Risk Reduction <http://archive-ouverte.unige.ch/unige:78299> (UNISDR,
606 2015).

607 Do, H. X., Mei, Y., & Gronewold, A. D.: To what extent are changes in flood magnitude
608 related to changes in precipitation extremes? *Geophysical Research Letters*, 47,
609 e2020GL088684. <https://doi.org/10.1029/2020GL088684>, 2020.

610 Fang, X. and Pomeroy, J.W.: Impact of antecedent conditions on simulations of a flood
611 in a mountain headwater basin. *Hydrological Processes*, 30(16), 2754-2772,
612 <https://doi:10.1002/hyp.10910>, 2016.

613 Feng, B. F., Dai M. L. and Zhang T.: Effect of Reservoir Group Joint Operation on
614 Flood Control in the Middle and Lower Reaches of Yangtze River, *Journal of*
615 *Water Resources Research* (3), 278-284, <https://doi:10.12677/JWRR.2017.63033>,
616 2017.

617 Fu, G., Yu, J., Yu, X., Ouyang, R., Zhang, Y., Wang, P., Liu, W. and Min, L.: Temporal
618 variation of extreme rainfall events in China, 1961-2009. *Journal of Hydrology*,
619 487, 48-59, <https://doi:10.1016/j.jhydrol.2013.02.021>, 2013.

620 Gao, T. and Xie, L.: Spatiotemporal changes in precipitation extremes over Yangtze
621 River basin, China, considering the rainfall shift in the late 1970s. *Global and*
622 *Planetary Change*, 147, 106-124, <https://doi:10.1016/j.gloplacha.2016.10.016>,
623 2016.

624 Gao, Y., Wang, H., Lu, X., Xu, Y., Zhang, Z. and Schmidt, A.R.: Hydrologic Impact
625 of Urbanization on Catchment and River System Downstream from Taihu Lake.
626 *Journal of Coastal Research*, 82-88, <https://doi:10.2112/SI84-012.1>, 2018.

627 Garg, S., & Mishra, V.: Role of extreme precipitation and initial hydrologic conditions
628 on floods in Godavari river basin, India. *Water Resources Research*, 55, 9191 –
629 9210. <https://doi.org/10.1029/2019WR025863>, 2019.

630 Grabs, T., Seibert, J., Bishop, K. and Laudon, H.: Modeling spatial patterns of saturated
631 areas: A comparison of the topographic wetness index and a dynamic distributed
632 model. *Journal of Hydrology*, 373(1-2), 15-23,
633 <https://doi:10.1016/j.jhydrol.2009.03.031>, 2009.

634 Huang, C., Zhou, Y., Zhang, S., Wang, J., Liu, F., Gong, C., Yi, C., Li, L., Zhou, H.,
635 Wei, L., Pan, X., Shao, C., Li, Y., Han, W., Yin, Z., and Li, X.: Groundwater
636 resources in the Yangtze River Basin and its current development and utilization[J].
637 *Geology of China*, 2021, 48(4):979-1000.

638 IPCC. *Managing the Risks of Extreme Events and Disasters to Advance Climate*
639 *Change Adaptation* (eds Field, C. B. et al.) (Cambridge Univ. Press, 2012).

640 Kato, K.: On the Abrupt Change in the Structure of the Baiu Front over the China
641 Continent in Late May of 1979. *Journal of the Meteorological Society of Japan*,
642 63(1), 20-36, https://doi:10.2151/jmsj1965.63.1_20, 1985.

643 Kazuki, T., Oliver C. S. V., Masahiro, R.: Spatial variability of precipitation and soil
644 moisture on the 2011 flood at chao phraya river basin. *International Water*
645 *Technology Association, Proceedings of Hydrology and Water Resources*, B, 17-
646 21, 2013.

647 Kemter, M., Merz, B., Marwan, N., Vorogushyn, S., & Blöschl, G.: Joint trends in flood
648 magnitudes and spatial extents across Europe. *Geophysical Research Letters*, 47,
649 e2020GL087464. <https://doi.org/10.1029/2020GL087464>, 2020.

650 Lehner, B., C. Reidy Liermann, C. Revenga, C. Vörösmarty, B. Fekete, P. Crouzet, P.
651 Döll, M. Endejan, K. Frenken, J. Magome, C. Nilsson, J.C. Robertson, R. Rodel,
652 N. Sindorf, and D. Wisser. 2011. High-resolution mapping of the world's
653 reservoirs and dams for sustainable river-flow management. *Frontiers in Ecology*
654 *and the Environment* 9 (9): 494-502.

655 Li, Q., Wei, F. and Li, D.: Interdecadal variation of East Asian summer monsoon and
656 drought/flood distribution over eastern China in the last 159 years. *Journal of*
657 *Geographical Sciences*, 21(4), 579-593, <https://doi:10.1007/s11442-011-0865-2>,
658 2011.

-
- 659 Li, X., Zhang, K., Gu, P., Feng, H., Yin, Y., Chen, W. and Cheng, B.: Changes in
660 precipitation extremes in the Yangtze River Basin during 1960-2019 and the
661 association with global warming, ENSO, and local effects. *Science of the Total*
662 *Environment*, 760, [https://doi:10.1016/j.scitotenv.2020.144244](https://doi.org/10.1016/j.scitotenv.2020.144244), 2021.
- 663 Liu, B., Yan, Y., Zhu, C., Ma, S., & Li, J.: Record - breaking Meiyu rainfall around the
664 Yangtze River in 2020 regulated by the subseasonal phase transition of the North
665 Atlantic Oscillation. *Geophysical Research Letters*, 47, e2020GL090342.
666 <https://doi.org/10.1029/2020GL090342>, 2020.
- 667 Liu, L., Ye, S., Chen, C., Pan, H. and Ran, Q.: Nonsequential Response in Mountainous
668 Areas of Southwest China. *Frontiers in Earth Science*, 9: 1-15. doi:
669 10.3389/feart.2021.660244, 2021
- 670 Liu, N., Jin, Y. and Dai, J.: Variation of Temperature and Precipitation in Urban
671 Agglomeration and Prevention Suggestion of Waterlogging in Middle and Lower
672 Reaches of Yangtze River. 3rd International Conference on Energy Equipment
673 Science and Engineering (Iceese 2017), 128, [https://doi:10.1088/1755-](https://doi.org/10.1088/1755-1315/128/1/012165)
674 [1315/128/1/012165](https://doi.org/10.1088/1755-1315/128/1/012165), 2018.
- 675 Liu, S., Huang, S., Xie, Y., Wang, H., Leng, G., Huang, Q., Wei, X., and Wang, L.:
676 Identification of the Non-stationarity of Floods: Changing Patterns, Causes, and
677 Implications, *Water Resour. Manag.*, 33, 939–953, 2018.
- 678 Liu, Y., Xinyu, L., Liancheng, Z., Yang, L., Chunrong, J., Ni, W. and Juan, Z.:
679 Quantifying rain, snow and glacier meltwater in river discharge during flood
680 events in the Manas River Basin, China. *Natural Hazards*, 108(1), 1137-1158,
681 [https://doi:10.1007/s11069-021-04723-8](https://doi.org/10.1007/s11069-021-04723-8), 2021.
- 682 Long, L.H., Ji, D.B., Yang, Z.Y., Cheng, H.Q., Yang, Z.J., Liu, D.F., Liu, L. and Lorke,
683 A.: Tributary oscillations generated by diurnal discharge regulation in Three
684 Gorges Reservoir. *Environmental Research Letters*, 15(8),
685 [https://doi:10.1088/1748-9326/ab8d80](https://doi.org/10.1088/1748-9326/ab8d80), 2020.
- 686 Lu, M., Wu, S.-J., Chen, J., Chen, C., Wen, Z. and Huang, Y.: Changes in extreme
687 precipitation in the Yangtze River basin and its association with global mean
688 temperature and ENSO. *International Journal of Climatology*, 38(4), 1989-2005,
689 [https://doi:10.1002/joc.5311](https://doi.org/10.1002/joc.5311), 2018.

690 Meles, M.B., Younger, S.E., Jackson, C.R., Du, E., Drover, D.: Wetness index based
691 on landscape position and topography (WILT): Modifying TWI to reflect
692 landscape position, *Journal of Environmental Management* 255, 109863, 2020.

693 Miao, Q., Huang, M. and Li, R., Q.: Response of net primary productivity of vegetation
694 in Yangtze River Basin to future climate change. *Journal of Natural Resources*, 25,
695 08(2010):1296-1305, doi:CNKI:SUN:ZRZX.0.2010-08-007, 2015.

696 Munoz, S.E., Giosan, L., Therrell, M.D., Remo, J.W.F., Shen, Z., Sullivan, R.M.,
697 Wiman, C., O'Donnell, M., and Donnelly, J.P.: Climatic control of Mississippi
698 River flood hazard amplified by river engineering, 556, 95 – 98, 2018.

699 Musselman, K.N., Lehner, F., Ikeda, K., Clark, M.P., Prein, A.F., Liu, C., Barlage, M.
700 and Rasmussen, R.: Projected increases and shifts in rain-on-snow flood risk over
701 western North America, *Nature Climate Change*, 8, 808 – 812, 2018.

702 Ockert J. G. and Jeff C. S.: Review of methods used to estimate catchment response
703 time for the purpose of peak discharge estimation, *Hydrological Sciences Journal*,
704 59:11, 1935-1971, DOI: 10.1080/02626667.2013.866712, 2014.

705 Ohmura, A. and Wild, M.: Is the hydrological cycle accelerating? *Science*, 298, 1345 –
706 1346, 2002.

707 Pegram, G. and Bardossy, A.: Downscaling Regional Circulation Model rainfall to
708 gauge sites using recorrelation and circulation pattern dependent quantile-quantile
709 transforms for quantifying climate change. *Journal of Hydrology*, 504, 142-159,
710 <https://doi:10.1016/j.jhydrol.2013.09.014>, 2013.

711 Peng, T., Tian, H., Singh, V. P., Chen, M., Liu, J., Ma, H. B. and Wang, J. B.:
712 Quantitative assessment of drivers of sediment load reduction in the Yangtze River
713 basin, China, *Journal of Hydrology*, 580,
714 <https://doi:10.1016/j.jhydrol.2019.124242>, 2020.

715 Qian, H. and Xu, S.-B.: Prediction of Autumn Precipitation over the Middle and Lower
716 Reaches of the Yangtze River Basin Based on Climate Indices. *Climate*, 8(4),
717 <https://doi:10.3390/cli8040053>, 2020.

718 Ran, Q., Chen, X., Hong Y., Ye S., and Gao J.: Impacts of terracing on hydrological
719 processes: A case study from the Loess Plateau of China. *Journal of Hydrology*,
720 588, <https://doi:10.1016/j.jhydrol.2020.125045>, 2020.

721 Ran, Q., Zong, X., Ye, S., Gao, J. and Hong, Y.: Dominant mechanism for annual
722 maximum flood and sediment events generation in the Yellow River basin. *Catena*,
723 187, <https://doi:10.1016/j.catena.2019.104376>, 2020.

724 Ray S. M., Ramakar J. and Kishanjit K. K.: Precipitation-runoff simulation for a
725 Himalayan River Basin, India using artificial neural network algorithms, *Sciences*
726 *in Cold and Arid Regions*, 5(1), 85-95, 2013.

727 Rottler, E., Francke, T., Burger, G., and Bronstert, A.: Long-term changes in central
728 European river discharge for 1869 – 2016: impact of changing snow covers,
729 reservoir constructions and an intensified hydrological cycle, *Hydrol. Earth Syst.*
730 *Sci.*, 24, 1721 – 1740, 2020.

731 Smith, J. A., Cox, A. A., Baeck, M. L., Yang, L., and Bates, P.: Strange floods: the
732 upper tail of flood peaks in the United States, *Water Resour. Res.*, 54, 6510 – 6542,
733 2018.

734 Sorensen, R., Zinko, U., and Seibert, J.: On the calculation of the topographic wetness
735 index: evaluation of different methods based on field observations, *Hydrology and*
736 *Earth System Sciences*, 10, 101–112, 2006.

737 Su, Z., Ho, M., Hao, Z., Lall, U., Sun, X., Chen, X. and Yan, L.: The impact of the
738 Three Gorges Dam on summer streamflow in the Yangtze River Basin.
739 *Hydrological Processes*, 34(3), 705-717, <https://doi:10.1002/hyp.13619>, 2020.

740 Suresh, S. S., Benefit O., Augustine T., and Trevor P.: Peoples' Perception on the
741 Effects of Floods in the Riverine Areas of Ogbia Local Government Area of
742 Bayelsa State, Nigeria, *Knowledge Management*, [https://doi:10.18848/2327-](https://doi:10.18848/2327-7998/CGP/v12i02/50793)
743 [7998/CGP/v12i02/50793](https://doi:10.18848/2327-7998/CGP/v12i02/50793), 2013.

744 Tao, S. Y., *Rainstorm in China* [M], Beijing: Science Press, 1980.(in Chinese)

745 Trambly, Y., Villarini, G., El Khalki, E. M., Gründemann, G., & Hughes, D.:
746 Evaluation of the drivers responsible for flooding in Africa. *Water Resources*
747 *Research*, 57, e2021WR029595. <https://doi.Org/10.1029/2021WR029595>, 2021.

748 USBR (United States Bureau of Reclamation), 1973. *Design of small dams*. 2nd ed.
749 Washington, DC: Water Resources Technical Publications.

750 Vicente-Serrano, S.M., Azorin-Molina, C., Sanchez-Lorenzo, A., Revuelto, J., Lopez-
751 Moreno, J.I., Gonzalez-Hidalgo, J.C., Moran-Tejeda, E. and Espejo, F.: Reference
752 evapotranspiration variability and trends in Spain, 1961-2011. *Global and*
753 *Planetary Change*, 121, 26-40, <https://doi:10.1016/j.gloplacha.2014.06.005>, 2014.

-
- 754 Volpi, E., Di Lazzaro, M., Bertola, M., Viglione, A. and Fiori, A.: Reservoir Effects on
755 Flood Peak Discharge at the Catchment Scale. *Water Resources Research*, 54(11),
756 9623-9636, <https://doi:10.1029/2018wr023866>, 2018.
- 757 Wang, H., Zhou, Y., Pang, Y. and Wang, X.: Fluctuation of Cadmium Load on a Tide-
758 Influenced Waterfront Lake in the Middle-Lower Reaches of the Yangtze River.
759 *Clean-Soil Air Water*, 42(10), 1402-1408, <https://doi:10.1002/clen.201300693>,
760 2014.
- 761 Wang, J., Ran, Q., Liu, L., Pan, H. and Ye, S.: Study on the Dominant Mechanism of
762 Extreme Flow Events in the Middle and Lower Reaches of the Yangtze River,
763 *China Rural Water and Hydropower*, Accepted.
- 764 Wang, R., Yao, Z., Liu, Z., Wu, S., Jiang, L. and Wang, L.: Snow cover variability and
765 snowmelt in a high-altitude ungauged catchment. *Hydrological Processes*, 29(17),
766 3665-3676, <https://doi:10.1002/hyp.10472>, 2015.
- 767 Wang, W., Xing W., Yang, T., Shao, Q., Peng, S., Yu, Z., and Yong, B.: Characterizing
768 the changing behaviours of precipitation concentration in the Yangtze River Basin,
769 China. *Hydrological Processes*, 27(24), 3375-3393, <https://doi:10.1002/hyp.9430>,
770 2013.
- 771 Wang, Z. and Plate, E.: Recent flood disasters in China. *Proceedings of the Institution*
772 *of Civil Engineers – Water and Maritime Engineering* (3),
773 <https://doi:10.1680/wame.2002.154.3.177>, 2002.
- 774 Wasko, C. and Nathan, R.: Influence of changes in rainfall and soil moisture on trends
775 in flooding. *Journal of Hydrology*, 575, 432-441,
776 <https://doi:10.1016/j.jhydrol.2019.05.054>, 2019.
- 777 Wasko, C., Nathan, R., & Peel, M. C.: Changes in antecedent soil moisture modulate
778 flood seasonality in a changing climate. *Water Resources Research*, 56,
779 e2019WR026300. <https://doi.org/10.1029/2019WR026300>, 2020.
- 780 Wasko, C., Nathan, R., Stein, L., O’Shea, D.: Evidence of shorter more extreme
781 rainfalls and increased flood variability under climate change. *J. Hydrol.* 603,
782 126994. <https://doi.org/10.1016/j.jhydrol.2021.126994>, 2021.
- 783 Wu, X. S., Guo, S. L. and Ba, H. H.: Long-term precipitation forecast method based on
784 SST multipole index, *Journal of water conservancy*(10), 1276-1283,
785 <https://doi:10.13243/j.cnki.slxb.20180544>, 2018.

-
- 786 Xia, J. and Chen, J.: A new era of flood control strategies from the perspective of
787 managing the 2020 Yangtze River flood. *Science China-Earth Sciences*, 64(1), 1-
788 9, <https://doi:10.1007/s11430-020-9699-8>, 2021.
- 789 Xie, Z., Du, Y., Zeng, Y. and Miao, Q.: Classification of yearly extreme precipitation
790 events and associated flood risk in the Yangtze-Huaihe River Valley. *Science*
791 *China-Earth Sciences*, 61(9), 1341-1356, <https://doi:10.1007/s11430-017-9212-8>,
792 2018.
- 793 Yang, H.F., Yang, S.L., Xu, K.H., Milliman, J.D., Wang, H., Yang, Z., Chen, Z. and
794 Zhang, C.Y.: Human impacts on sediment in the Yangtze River: A review and new
795 perspectives. *Global and Planetary Change*, 162, 8-17,
796 <https://doi:10.1016/j.gloplacha.2018.01.001>, 2018.
- 797 Yang, L., Wang, L., Li, X. and Gao, J.: On the flood peak distributions over China.
798 *Hydrology and Earth System Sciences*, 23(12), 5133-5149,
799 <https://doi:10.5194/hess-23-5133-2019>, 2019.
- 800 Yang, W., Yang, H., and Yang, D.: Classifying floods by quantifying driver
801 contributions in the Eastern Monsoon Region of China, *Journal of Hydrology*, 585,
802 124767, 2020.
- 803 Yang, W., Yang, H., Yang, D., and Hou, A.: Causal effects of dams and land cover
804 changes on flood changes in mainland China. *Hydrol. Earth Syst. Sci.*, 25, 2705–
805 2720, 2021.
- 806 Ye, S., Li, H., Leung, L.R., Guo, J., Ran, Q., Demissie, Y., et al., 2017. Understanding
807 flood seasonality and its temporal shifts within the contiguous United States. *J.*
808 *Hydrometeorol.* 18 (7), 1997 – 2009.
- 809 Ye, X., Xu, C.-Y., Li, Y., Li, X. and Zhang, Q.: Change of annual extreme water levels
810 and correlation with river discharges in the middle-lower Yangtze River:
811 Characteristics and possible affecting factors. *Chinese Geographical*
812 *Science*, 27(2), 325-336, <https://doi:10.1007/s11769-017-0866-x>, 2017.
- 813 Yu, F., Chen, Z., Ren, X. and Yang, G.: Analysis of historical floods on the Yangtze
814 River, China: Characteristics and explanations. *Geomorphology*, 113(3-4), 210-
815 216, <https://doi:10.1016/j.geomorph.2009.03.008>, 2009.
- 816 Zhang, H., Liu, S., Ye, J. and Yeh, P.J.F.: Model simulations of potential contribution
817 of the proposed Huangpu Gate to flood control in the Lake Taihu basin of China.

818 Hydrology and Earth System Sciences, 21(10), 5339-5355,
819 <https://doi:10.5194/hess-21-5339-2017>, 2017.

820 Zhao, J., Li, J., Yan, H., Zheng, L. and Dai, Z.: Analysis on the Water Exchange
821 between the Main Stream of the Yangtze River and the Poyang Lake. 2011 3rd
822 International Conference on Environmental Science and Information Application
823 Technology Esiat 2011, Vol 10, Pt C,10, 2256-2264,
824 <https://doi:10.1016/j.proenv.2011.09.353>, 2011.

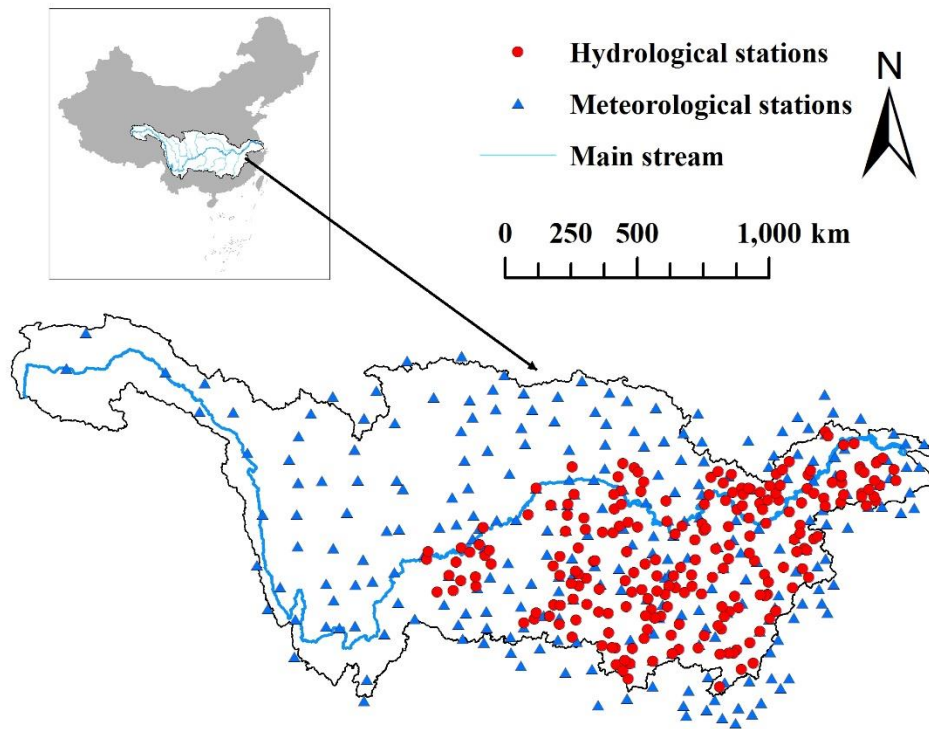
825 Zhang, S., Kang, L. and He, X.: Equal proportion flood retention strategy for the leading
826 multireservoir system in upper Yangtze River. International Conference on Water
827 Resources and Environment, WRE 2015, 2015.

828 Zhang, W., Villarini, G., Vecchi, G.A. and Smith, J. A.: Urbanization exacerbated the
829 rainfall and flooding caused by hurricane Harvey in Houston. *Nature*, 563, 384 –
830 388, 2018.

831 Zhang, K., Wang, Q., Chao, L., Ye, J., Li, Z., Yu, Z., Yang, T. and Ju, Q.: Ground
832 observation-based analysis of soil moisture spatiotemporal variability across a
833 humid to semi-humid transitional zone in China. *Journal of Hydrology*, 574, 903-
834 914, 2019.

835 Zou, B., Li, Y., Feng, B.: Analysis on dispatching influence of Three Gorges Reservoir
836 on water level of main stream in mid-lower reaches of Yangtze River: a case study
837 of flood in July,2010. *Yangtze River*, 42.06:80-82+100. doi:10.16232/j.cnki.1001-
838 4179.2011.06.004, 2011.

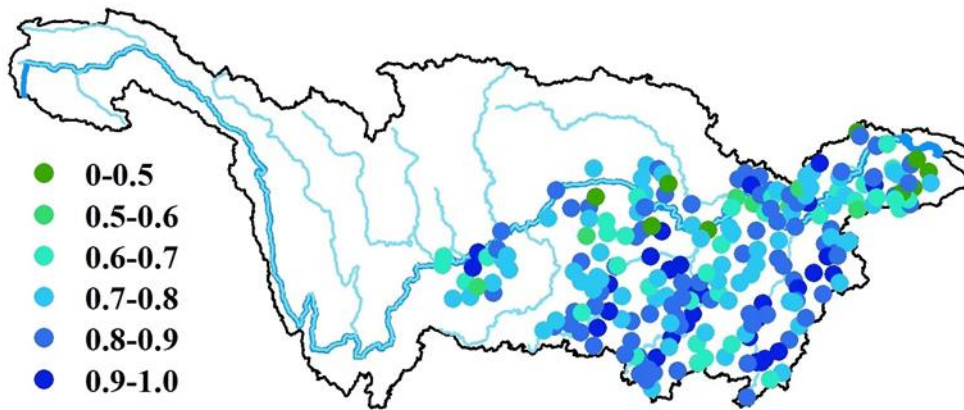
839
840



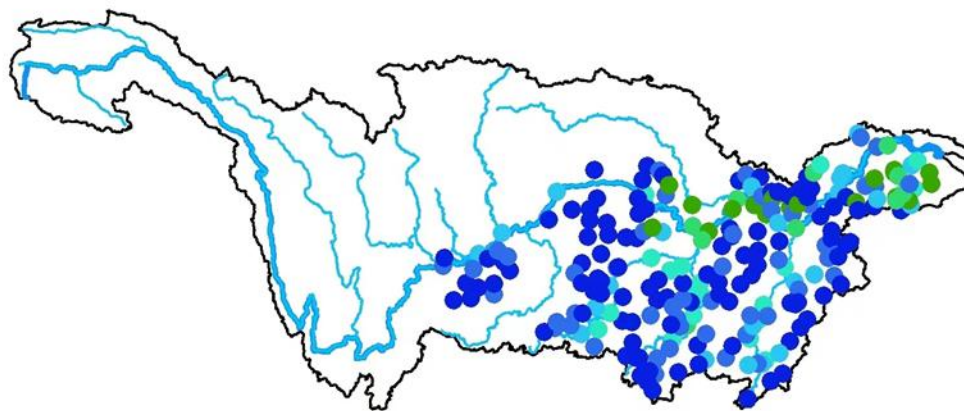
841

842 **Figure 1:** Map of the Yangtze River basin, and the meteorological stations and
843 hydrological stations. The blue line is the main stream of Yangtze River.

844



(a) Percentile of antecedent soil moisture

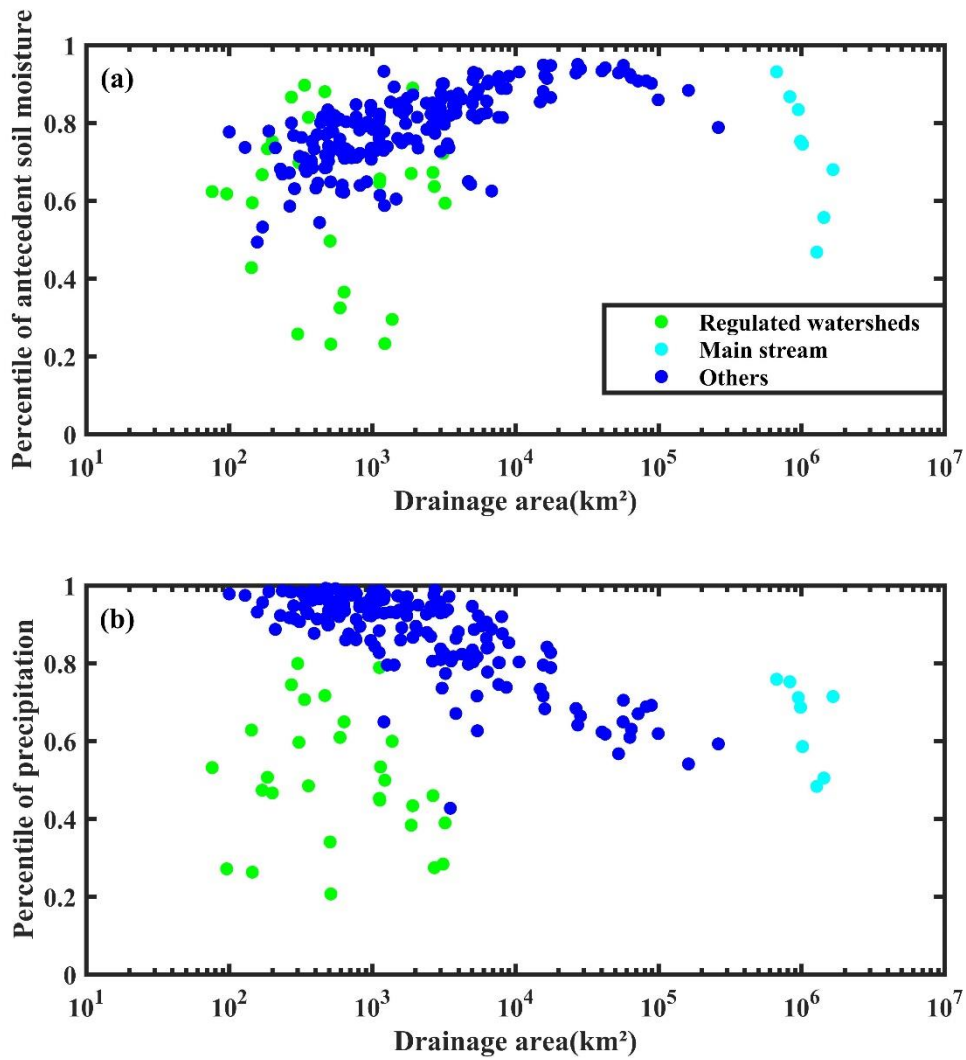


(b) Percentile of precipitation

845

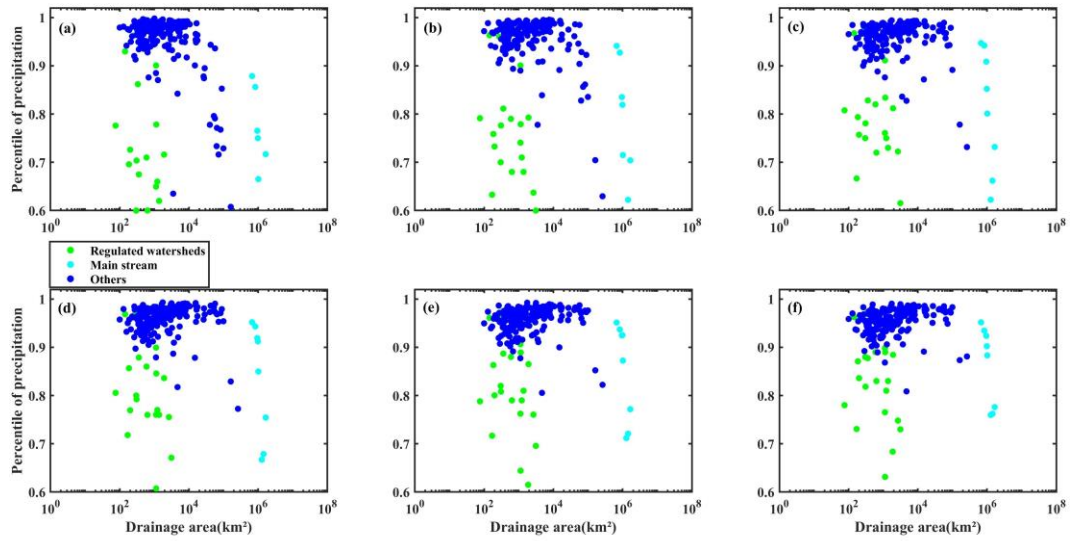
846 **Figure 2:** The spatial distribution of (a) the percentile of antecedent soil moisture during
 847 annual maximum flood; (b) the percentile of daily precipitation during annual
 848 maximum flood.

849



850
 851 **Figure 3:** Scatterplot between the drainage area and (a) the percentile of antecedent soil
 852 moisture of AMF events (the linear regression for blue dots: $R^2 = 0.46$, p -value <0.001);
 853 (b) the percentile of precipitation at the day of AMF events (the linear regression for
 854 blue dots: $R^2 = 0.61$, p -value <0.001). The green dots represent the regulated watershed,
 855 the cyan dots represent the sites on the main stream, and the rest sites are shown in blue.

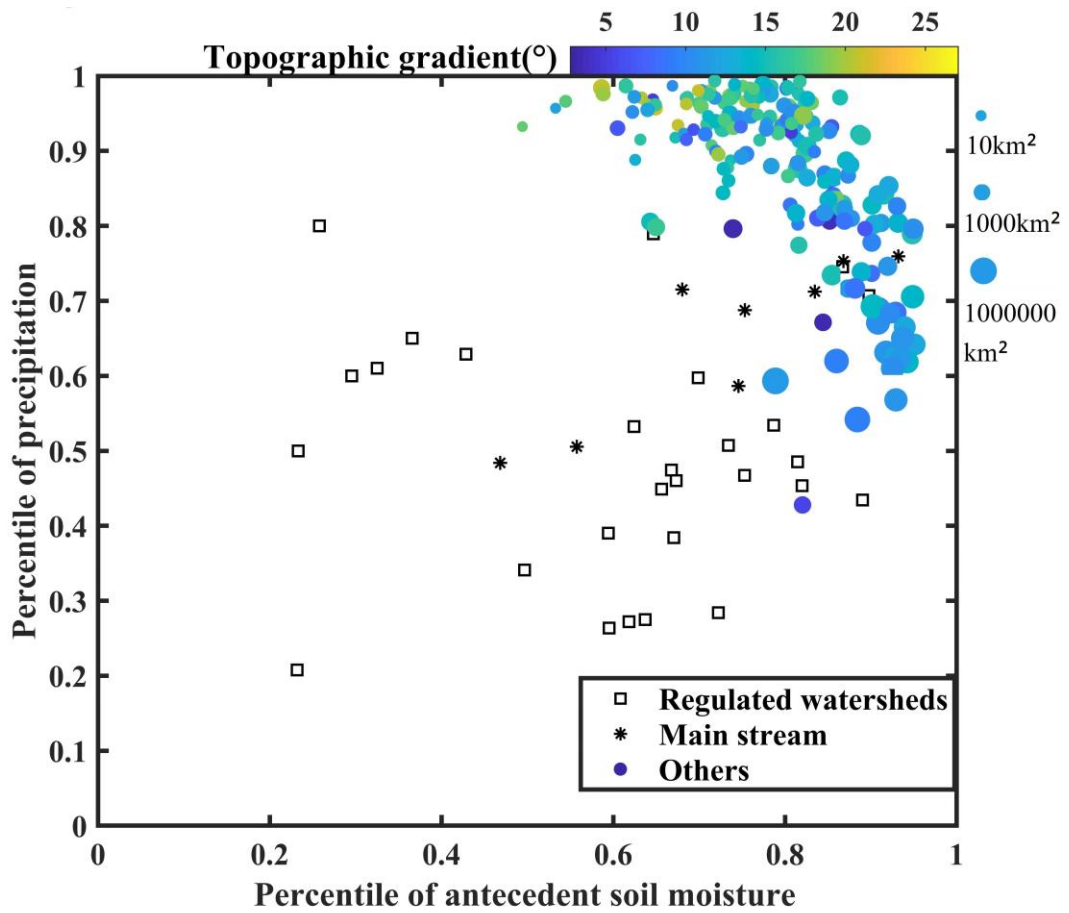
856
 857
 858



859

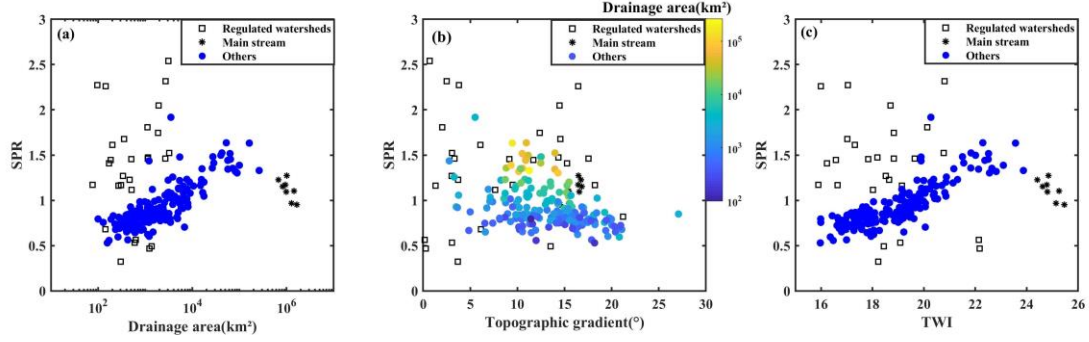
860 **Figure 4:** Scatterplot between the drainage area and the percentile of accumulated
 861 rainfall of (a) two days; (b) three days; (c) four days; (d) five days; (e) six days; and (f)
 862 seven days on AMF events.

863



864
 865
 866
 867
 868

Figure 5: Scatterplot of the percentile of precipitation and antecedent soil moisture, the color represents topographic gradient and the size of circles is scaled by drainage area.



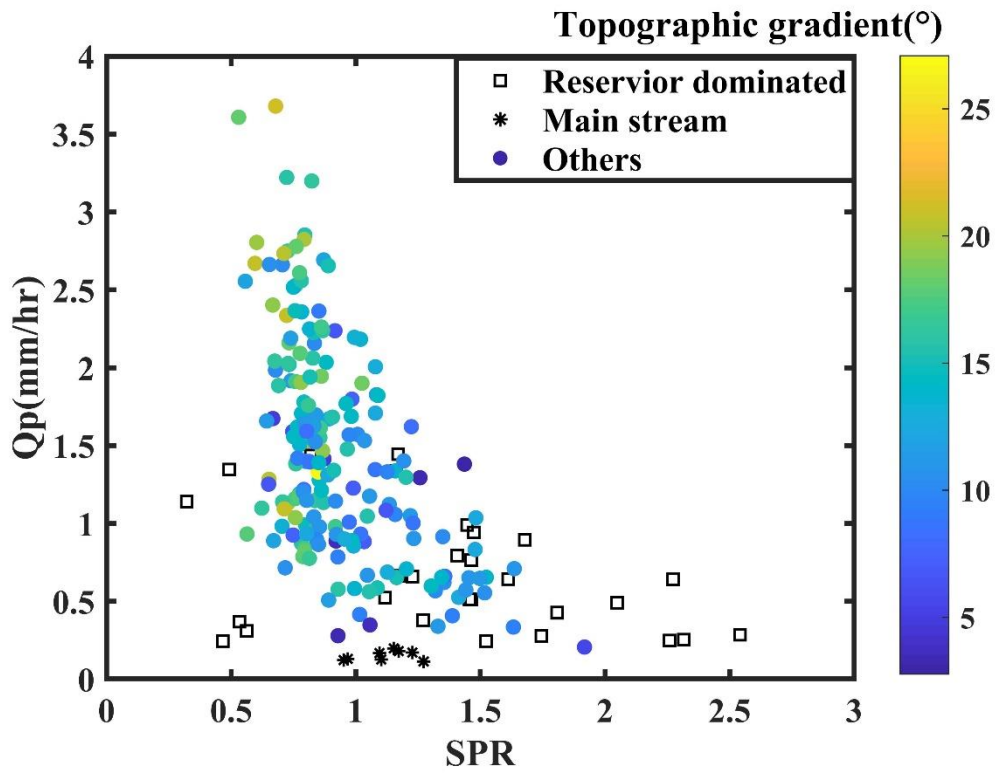
869

870 **Figure 6:** Scatterplots between the ratio of antecedent soil moisture and precipitation

871 (SPR) and (a) drainage area; (b) topographic gradient; and (c) topographic wetness

872 index (TWI).

873



874

875 **Figure 7:** Scatterplot between the ratio of antecedent soil moisture and precipitation
876 (SPR) and area weighted annual maximum discharge (Q_p), the color represents
877 topographic gradient.

878

Supplementary

1
2 To validate our results, we collected the 0-200cm soil moisture from the China Land
3 Data Assimilation System (CLDAS) provided by China Meteorological Administration
4 (CMA) (Wang & Li 2020). 37 catchments covering a range of climate and topography
5 were selected for comparison (Figure S3). Since this dataset only has soil moisture data
6 from 2008, the mean percentile of antecedent soil moisture was calculated from 2008
7 to 2016 based on the CLDAS soil moisture. This was then compared with the mean
8 percentile based on water balance as in the manuscript (Figure S4). As we can see from
9 Figure S4, the scatters fall around the 1:1 line, that is, the mean percentile calculated
10 from water balance are close to the mean percentile from re-analysis soil moisture. This
11 is consistent with our discussion that averaging through long-term records would be
12 less impacted by the simplification in estimation. Due to the length of CLDAS dataset,
13 we only averaged within 9 years, for the at least 25 years records used in our study, it
14 is likely to be less scatter. While this is just a minimal evaluation of the values, given
15 the goal of this study, we think the averaged percentile of antecedent soil moisture based
16 on the water balance model is acceptable for the purpose of this study at the mean
17 annual scale.

18
19 Wang, Y. and Li, G. (2020). Evaluation of simulated soil moisture from China Land Data
20 Assimilation System (CLDAS) land surface models, *Remote Sensing Letters*, 11 (12),
21 1060 – 1069.

25 **Table S1:** Estimated concentration time for 10 sites with largest drainage area: the ones
26 on main stream (MS) and the ones at the outlets of major tributaries (TR).

27

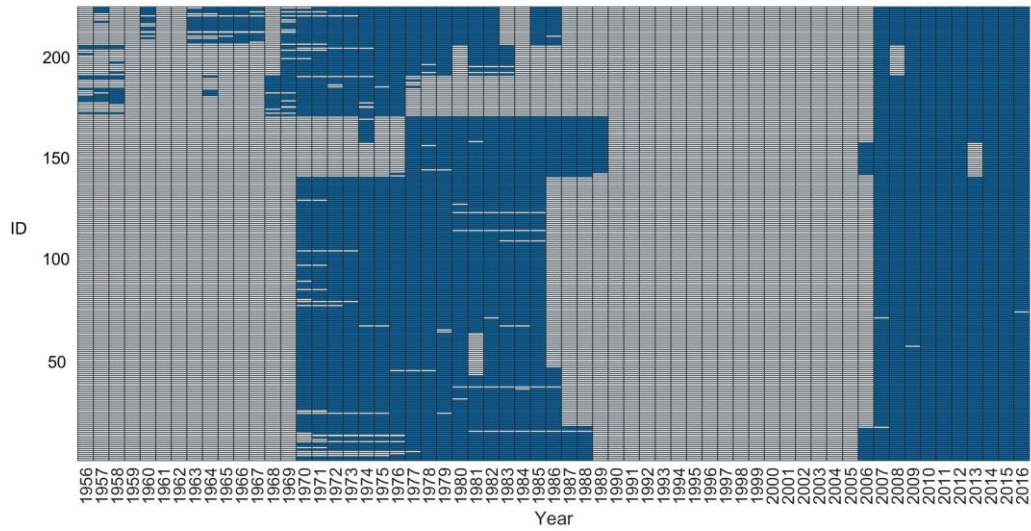
Site Name	Concentration Time (hr)	Drainage Area (km ²)
TR-Hukou	17.9	161,979
TR-Chenglingji	18.8	261,986
MS-Zhutuo	32.7	668,661
MS-Cuntan	32.8	827,799
MS-Wanxian	37.6	948,524
MS-Yichang	41.5	982,948
MS-Jianli	45.2	1,014,690
MS-Luoshan	46.3	1,276,676
MS-Hankou	51.0	1,432,008
MS-Datong	54.3	1,657,604

28

29

30

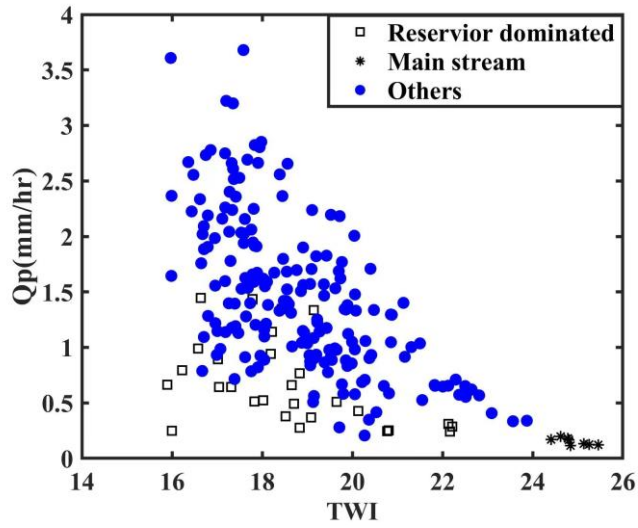
31



32

33 **Figure S1:** The data availability of each station, each column indicates each year while
 34 each row is corresponding to each station, blue grid indicates there is record of this year.

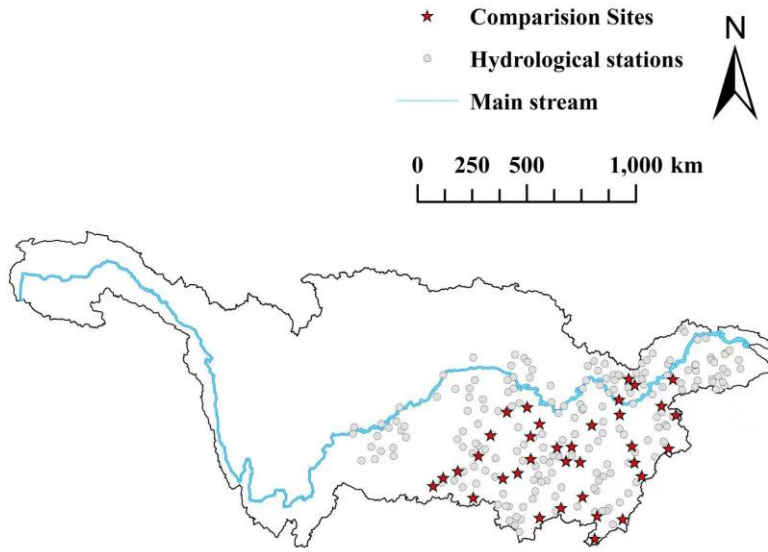
35



36

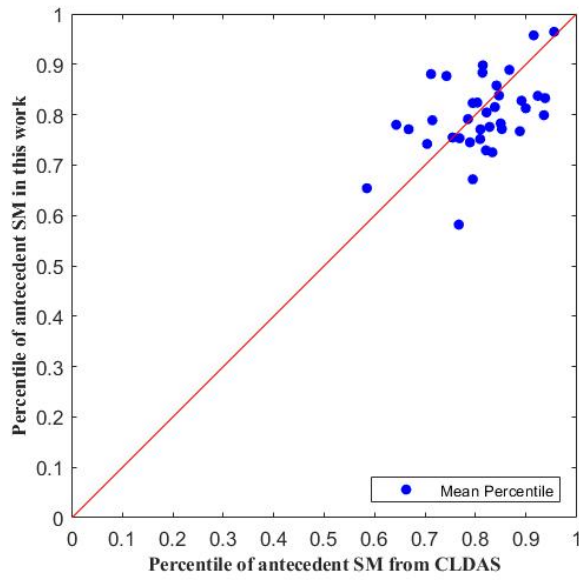
37 **Figure S2:** Scatterplot between the topographic wetness index (TWI) and area weighted
38 annual maximum discharge (Q_P).

39



40
41
42

Figure S3: Map of the 37 selected stations used for comparison.



43
44
45
46
47
48
49

Figure S4: Comparison between the mean percentile of antecedent soil moisture in our work and the percentile of antecedent soil moisture from re-analysis dataset CLDAS (China Land Data Assimilation System). The red line is the 1:1 line.